

April 1991

Effect of interfacial microstructure on magnetic properties of dysprosium multilayers

Z.S. Shan

University of Nebraska - Lincoln

B. Jacobsen

University of Nebraska - Lincoln

Sy_Hwang Liou

University of Nebraska-Lincoln, sliou@unl.edu

David J. Sellmyer

University of Nebraska-Lincoln, dsellmyer@unl.edu

Follow this and additional works at: <http://digitalcommons.unl.edu/physicsliou>



Part of the [Physics Commons](#)

Shan, Z.S.; Jacobsen, B.; Liou, Sy_Hwang; and Sellmyer, David J., "Effect of interfacial microstructure on magnetic properties of dysprosium multilayers" (1991). *Si-Hwang Liou Publications*. 43.
<http://digitalcommons.unl.edu/physicsliou/43>

This Article is brought to you for free and open access by the Research Papers in Physics and Astronomy at DigitalCommons@University of Nebraska - Lincoln. It has been accepted for inclusion in Si-Hwang Liou Publications by an authorized administrator of DigitalCommons@University of Nebraska - Lincoln.

Effect of interfacial microstructure on magnetic properties of dysprosium multilayers

Z. S. Shan,^{a)} B. Jacobsen, S. H. Liou, and D. J. Sellmyer

Behlen Laboratory of Physics and Center for Materials Research and Analysis, University of Nebraska, Lincoln, Nebraska 68588-0111

Nanostructured multilayers of Dy/M (M = Ta, Cu, Y, and Co) have been investigated. Correlations between the microstructure and the magnetic properties, in particular the effects of interfacial structure, are discussed. The temperature and layer-thickness dependences of anisotropy of these Dy/M multilayers can be interpreted reasonably in light of the model previously developed for the perpendicular anisotropy in amorphous multilayers.

I. INTRODUCTION

The perpendicular magnetic anisotropy (PMA) in compositionally modulated films (CMF) has been a subject of considerable interest in recent years. However, it is generally difficult to determine the origin of PMA because it may originate from various sources, such as magnetic dipolar interaction,¹ single-ion anisotropy,² magnetostrictive anisotropy,³ etc., all of which are related to the anisotropic pair correlations of the constituent atoms. Fortunately, the $4f$ -electrons of rare earth (RE) ions, which are responsible for the magnetic moments, are well localized, and thus the single-ion anisotropy is directly related to the crystal field acting on the moments and can be described in a rather simple way.⁴ In our previous work, we have developed an analytical model^{5,6} (hereafter denoted as the model) to understand the magnetic properties of amorphous, sinusoidally modulated RE/TM CMF (RE = Dy, Tb; TM = Fe, Co). Similarly, Baczewski *et al.* have analyzed the PMA of Nd/Fe and Tm/Fe CMF on the basis of calculating the crystal-field assuming ideal sharp interfaces.⁷

The main conclusion of the model is that the relationship between the intrinsic anisotropy K_u , the distributions of RE-subnetwork magnetization and constituent atoms can be expressed as

$$K_u = \xi \langle M_{RE}(z)^2 \rangle (A/\lambda) \quad (1)$$

for a CMF with thin layer thicknesses, where A is the peak-to-peak compositional modulation of the constituents, $\langle M_{RE}(z)^2 \rangle$ is the statistical average of RE-subnetwork magnetization squared over the whole sample, ξ is a parameter which is related to the anisotropic short-range order, ion radius and charge number of constituent ions, and λ is the bilayer thickness.

As we have discussed previously^{5,6} this expression shows: (1) Since (A/λ) can be interpreted as an average compositional gradient of the constituent atoms, then the sharper boundary favors a larger PMA. (2) The larger the M_{RE} , the larger the PMA. (3) The value of ξ changes from one RE/TM series of samples to another. However, it can be regarded as a constant for one series of samples.

This paper is an extension of our previous work, especially to the RE/NM CMF (NM is the nonmagnetic metal Ta, Cu, and Y), to further investigate the applicability of the model to cases when the magnetization comes wholly from the RE subnetwork.

II. EXPERIMENTS

The samples of $X \text{ \AA} \text{ Dy}/6 \text{ \AA} \text{ NM}$ ($X = 3.5, 5.25, 7, 10.5, 14, 21$; NM = Ta, Cu, Y), and $X \text{ \AA} \text{ Dy}/6 \text{ \AA} \text{ Co}$ ($X = 3.5, 5, 8, 11, 14$) were prepared with a multiple-gun sputtering system and the preparation conditions are same as those mentioned in Ref. 8. The structural properties were studied with small- and large-angle x-ray diffractions and the magnetic properties were measured with SQUID and vibrating sample magnetometers at room and low temperature.

III. RESULTS AND DISCUSSION

A. Interface sharpness and crystalline structure

Characterization of the layered structure of the samples was made by means of small-angle x-ray diffraction. One example for $14 \text{ \AA} \text{ Dy}/6 \text{ \AA} \text{ Ta}$ and $7 \text{ \AA} \text{ Dy}/6 \text{ \AA} \text{ Ta}$ samples is shown in Fig. 1(a). Sample $14 \text{ \AA} \text{ Dy}/6 \text{ \AA} \text{ Ta}$ shows both first- and second-order peaks, and sample $7 \text{ \AA} \text{ Dy}/6 \text{ \AA} \text{ Ta}$ only shows the first-order peak, i.e., the former has the sharper interface and both have the layered structure. The small-angle x-ray diffraction for Dy/Ta, Dy/Co, Dy/Cu and Dy/Y indicates that their interface sharpness decrease in order: second-order peak for Dy/Ta, only first-order peak for Dy/Co, and no peak at all for Dy/Cu and Dy/Y for individual layer thickness of about 14 \AA . The crystalline structure was measured with large-angle x-ray diffraction and one example for the same samples is given in Fig. 1(b). Sample $14 \text{ \AA} \text{ Dy}/6 \text{ \AA} \text{ Ta}$ shows microcrystalline order, but $7 \text{ \AA} \text{ Dy}/6 \text{ \AA} \text{ Ta}$ has an amorphous structure. The large-angle x-ray diffraction shows similar results for Dy/Co and Dy/Cu. But Dy/Y shows sharp diffraction peaks for $7 \text{ \AA} \text{ Dy}/6 \text{ \AA} \text{ Y}$, i.e., crystalline order, because both Dy and Y have the hcp structure and very similar lattice constants.

B. Temperature dependence of magnetic properties

The temperature dependence of magnetization for $5.25 \text{ \AA} \text{ Dy}/6 \text{ \AA} \text{ NM}$ (NM = Ta, Y) are manifested in Fig. 2.

^{a)}Permanent address: Dept. of Electronic Engineering, Hangzhou University, Hangzhou, Zhejiang, People's Republic of China.

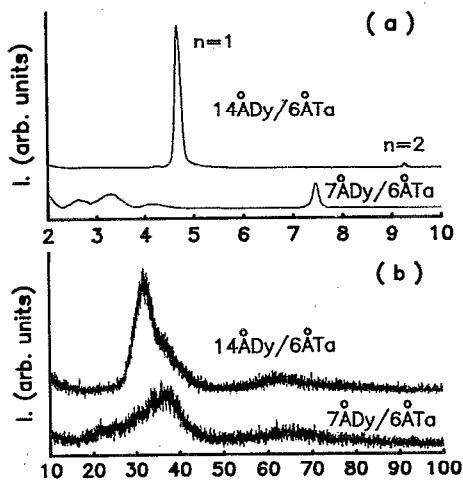


FIG. 1. X-ray diffraction intensity as a function of 2θ for 14 \AA Dy/ 6 \AA Ta and 7 \AA Dy/ 6 \AA Ta CMF. The small-angle patterns is in (a), and the large-angle patterns in (b).

Because Ta and Y are nonmagnetic, all the magnetization comes from Dy, but the magnetization value is strongly affected by the NM atoms. As the temperature increases, the magnetizations first decrease rapidly and then gradually.

One example of the temperature dependence of hysteresis loops for 5.25 \AA Dy/ 6 \AA Ta is shown in Fig. 3. It is seen that this sample demonstrates weak perpendicular anisotropy at 5 K and in-plane anisotropy at higher temperature since the sample has larger Dy magnetization at lower temperature. At room temperature the sample shows paramagnetism.

Comparing with the Dy/NM CMF, the Dy/Co CMF exhibit much stronger temperature dependence of anisotropy. Figure 4 shows the magnetic properties for $X \text{ \AA}$ Dy/ 6 \AA Co ($X = 3.5, 5, 8, 11, 14$) at 300 and 4.2 K. It is seen clearly: (1) The intrinsic anisotropy K_u is much larger at 4.2 K than at 300 K. For example, the maximum K_u is about $1.4 \times 10^7 \text{ erg/cm}^3$ at 4.2 K and only $2 \times 10^6 \text{ erg/cm}^3$

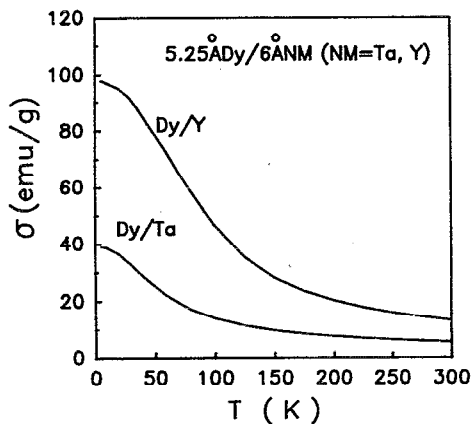


FIG. 2. Temperature dependence of magnetization at $H = 55 \text{ kOe}$ for 5.25 \AA Dy/ 6 \AA Ta and 5.25 \AA Dy/ 6 \AA Y CMF.

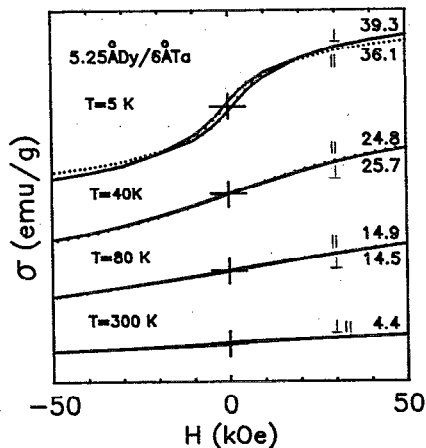


FIG. 3. Temperature dependence of hysteresis loops for 5.25 \AA Dy/ 6 \AA Ta ($T = 5, 40, 80, 300 \text{ K}$).

at 300 K. This is attributed to the fact that the single-ion anisotropy of Dy ion is proportional to its magnetization squared which is well ordered at 4.2 K. (2) Both at 4.2 and 300 K, sample 5 \AA Dy/ 6 \AA Co, whose individual layer thickness of Dy and Co are about 2-atomic layers, has the maximum values of anisotropy. This feature can be understood in terms of Eq. (1): the individual layer thickness of about 2-atomic layers may show the largest anisotropic distribution of constituent atoms, i.e., the largest value of (A/λ) . (3) In this figure, the net magnetization σ is expressed as $\sigma = \sigma_{\text{Co}} - \sigma_{\text{Dy}}$, where σ_{Co} and σ_{Dy} are the magnetizations of Co and Dy subnetworks, respectively. We notice that at the compensation points where $\sigma = 0$ at 300 or 4.2 K, the intrinsic anisotropy K_u has a rather large value. This implies that not the total magnetization, but the Dy-subnetwork magnetization gives the major contribution to the anisotropy. All these three points are explained by the model reasonably.

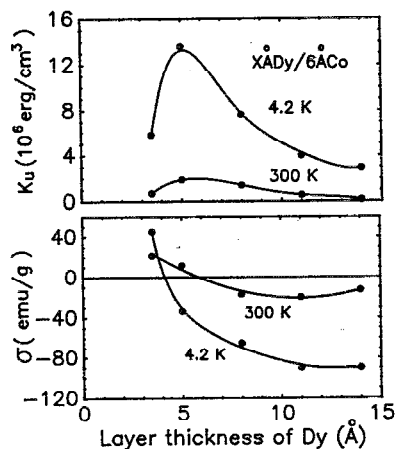


FIG. 4. Anisotropy and magnetization for $X \text{ \AA}$ Dy/ 6 \AA Co ($X = 3.5, 5, 8, 10$) at 300 and 4.2 K.

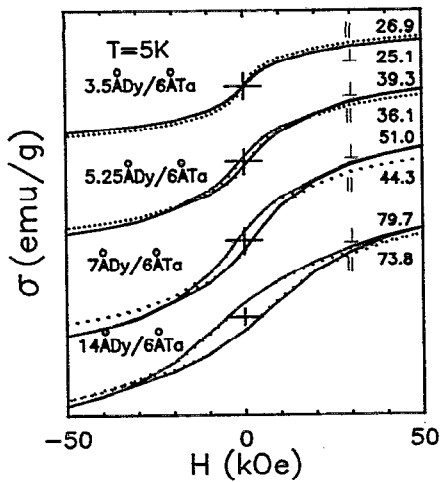


FIG. 5. Layer-thickness dependence of hysteresis loops for $X \text{ \AA} \text{ Dy}/6 \text{ \AA} \text{ Ta}$ ($X = 3.5, 5.25, 7, 14$) at $T = 5 \text{ K}$.

C. Layer-thickness dependence of magnetic properties

Two examples of layer-thickness dependence of hysteresis loops are shown in Figs. 5 and 6 for $X \text{ \AA} \text{ Dy}/6 \text{ \AA} \text{ Ta}$ and $X \text{ \AA} \text{ Dy}/6 \text{ \AA} \text{ Y}$ ($X = 3.5, 5.25, 7, 14$), respectively. Because both series of samples are disordered magnetically at room temperature, the measurements are performed at $T = 5 \text{ K}$. We notice: (1) For $X \text{ \AA} \text{ Dy}/6 \text{ \AA} \text{ Ta}$ samples, $\sigma_{\perp} < \sigma_{\parallel}$ for $X = 3.5$ and $\sigma_{\perp} > \sigma_{\parallel}$ for $X = 5.25, 7$, and 14 . As the Dy layer thickness increases, the PMA decreases (not shown in this figure). This can be approximately understood as following from the layer-thickness dependence of (A/λ) , which is dominated by A at small X and by λ at larger X . Figure 6 shows that all $X \text{ \AA} \text{ Dy}/6 \text{ \AA} \text{ Y}$ samples have $\sigma_{\parallel} > \sigma_{\perp}$, i. e., in-plane anisotropy, and the both $\sigma_{\parallel}(H)$ and $\sigma_{\perp}(H)$ manifest broad loops. This behavior may be

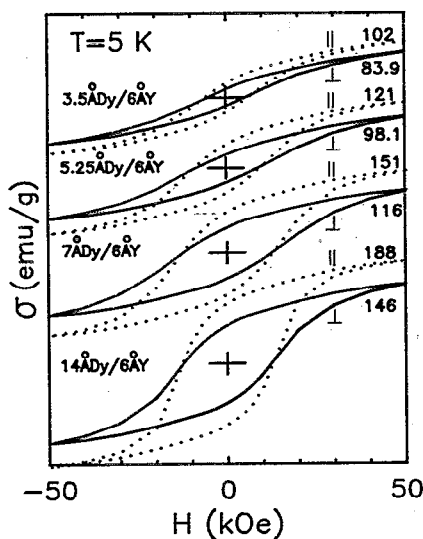


FIG. 6. Layer-thickness dependence of hysteresis loops for $X \text{ \AA} \text{ Dy}/6 \text{ \AA} \text{ Y}$ ($X = 3.5, 5.25, 7, 14$) at $T = 5 \text{ K}$.

accounted for by the structure of these samples, which is a disordered, crystalline hcp structure with the c -axes mainly normal to the film plane. For DyY crystalline alloys, the easy axis is known to be in the basal plane which is consistent with result of Fig. 6. In addition, the large coercive fields ($\sim 12 \text{ kOe}$) and $\sigma(H)$ behavior suggest that there may well be fluctuations among the Dy-Dy exchange interactions leading to aspects of spin-glass-like order.

In contrast with Dy/NM CMF which is only ordered magnetically at low temperature, the Dy/Co CMF (see Fig. 1 in Ref. 5) is ordered at room temperature. This figure shows an example of the layer-thickness dependence of hysteresis loops for $n(3.5 \text{ \AA} \text{ Dy}/2.5 \text{ \AA} \text{ Co})$ ($n = 1, 1.5, 2, 3, 6$). It is seen clearly that the samples with thinner layer thickness ($1.5 < n < 3$) exhibit perpendicular anisotropy because the interfacial region plays a dominant role and the samples with thicker layer thickness ($n > 6$) have the in-plane anisotropy because the inner region of Co plays a dominant role. It is worthy of mention that samples with $n = 1.5, 2$, and 3 show large PMA, just where the individual layer thicknesses of Dy and Co are about two atomic layers and consequently these samples have the largest (A/λ) .

IV. SUMMARY

In summary, the single-ion anisotropy of the RE ions with orbital angular momentum is the major origin of PMA and the interfacial region gives the main contribution. The PMA is weaker for Dy/NM CMF as compared to Dy/Co because the exchange fields of the former cause M_{RE}^2 to be much smaller. These results can be understood in terms of the model we have developed.

ACKNOWLEDGMENTS

We are grateful for financial support of NSF under Grant No. DMR-8918889. We thank S. Nafis, A. Nazareth, D. X. Wang, and J. X. Shen for assistance and helpful discussions.

- ¹T. Mizoguchi, and G. S. Cagill, *J. Appl. Phys.* **50**, 3570 (1979).
- ²Y. Suzuki, S. Takyma, F. Kirino, and N. Ohta, *IEEE Trans. Magn.* **23**, 2275 (1987).
- ³C. H. Lee, H. He, F. J. Lamelas, W. Vavra, C. Uher, and R. Clark, *Phys. Rev. B* (to be published); H. He, C. H. Lee, F. J. Lamelas, W. Vavra, D. Barlett, and R. Clarke, *J. Appl. Phys.* **67**, 5412 (1990).
- ⁴A. Fert, *Proc. NATO Advanced Study Institute, Crete, Greece* (to be published).
- ⁵Z. S. Shan, D. J. Sellmyer, S. S. Jaswal, Y. J. Wang, and J. X. Shen, *Phys. Rev. Lett.* **63**, 449 (1989).
- ⁶Z. S. Shan, Ph.D dissertation, University of Nebraska, 1990. Z. S. Shan, D. J. Sellmyer, S. S. Jaswal, Y. J. Wang, and J. X. Shen, *Phys. Rev. B* **42**, 10446 (1990).
- ⁷L. T. Baczkowski, M. Piecuch, J. Durand, G. Marchal, and P. Delcroix, *Phys. Rev. B* **40**, 11237 (1980).
- ⁸Z. S. Shan, S. Nafis, K. D. Aylesworth, and D. J. Sellmyer, *J. Appl. Phys.* **63**, 3218 (1988); Z. S. Shan, and D. J. Sellmyer, *J. Appl. Phys.* **67**, 5713 (1990).